Article

J. Biol. Regul. Homeost. Agents. 2024; 38(5): 3791–3801
https://doi.org/10.23812/j.biol.regul.homeost.agents.20243805.299

PROM1 Upregulation in Renal Tubular Epithelial Cells Regulates PFKFB3-Driven Glycolysis through the mTORC1 Pathway to Improve Renal Fibrosis

Tiantian Shi[1,†], Huijing Yue[1,†], Mei Cheng[2], Chen Yang[1,*]

[1]Department of Nephrology, Shiyan Renmin Hospital, 442000, Shiyan, Hubei, China
[2]Department of Internal Medicine, Sinopharm Dongfeng Maojian Hospital, Shiyan Mental Hospital, 442000, Shiyan, Hubei, China
*Correspondence: syyangchen@126.com (Chen Yang)
[†]These authors contributed equally.
Published: 1 May 2024

Background: Renal fibrosis is a common pathological alteration in chronic kidney disease (CKD), in which prominin 1 (PROM1) serves as a hub signature, as confirmed by a weighted gene co-expression network analysis. This study aims to investigate the precise function and mechanism of PROM1 in renal fibrosis.
Methods: The *in vivo* and *in vitro* models of renal fibrosis were established by inducing overexpression of PROM1 in unilateral ureteric obstruction (UUO) mice and transforming growth factor-β (TGF-β)-treated HK-2 cells (renal tubular epithelial cells). Mammalian target of rapamycin complex 1 (mTORC1) activator MHY1485 was used in rescue experiments *in vitro*. Expressions of PROM1 and proteins relevant to fibrosis, the mTORC1 pathway, and glycolysis in animal and cell models were determined using western blot. Kidney fibrosis and injury, as well as 6-phosphofructo-2-kinase/fructose-2,6-bisphosphatase 3 (PFKFB3) location were observed following tissue staining. Lactate content and extracellular acidification rate (ECAR) were measured to assess cellular glycolysis level.
Results: PROM1 was lowly expressed in kidneys and its overexpression improved kidney fibrosis of UUO mice. PROM1 overexpression rescued TGF-β-induced fibroid transformation, lactate accumulation, and ECAR increase in HK-2 cells. PROM1 overexpression reversed upregulation of fibronectin (FN), type I collagen (COL-I), plasminogen activator inhibitor-1 (PAI-1), mTOR, Raptor, Rictor, phosphorylated S6 ribosomal protein (p-S6), hexokinase 2 (HK2), and PFKFB3 in kidneys of UUO mice and TGF-β-treated HK-2 cells. MHY1485 generated opposite effects on TGF-β-treated HK-2 cells, and weakened the effects of PROM1 overexpression on suppression of the mTORC1 pathway and glycolysis.
Conclusion: PROM1 upregulation in renal tubular epithelial cells regulates PFKFB3-driven glycolysis through the mTORC1 pathway to improve renal fibrosis. Our results suggest that PROM1 is a promising therapeutic target for CKD prevention and treatment.

Keywords: prominin 1; mammalian target of rapamycin complex 1; renal fibrosis; glycolysis; 6-phosphofructo-2-kinase/fructose-2,6-bisphosphatase 3

Introduction

Chronic kidney disease (CKD) has a high fatality rate worldwide, and is one of the few non-communicable diseases with rising mortality over the past 20 years. More than 800 million individuals are suffering from CKD, accounting for 10% of the general population globally [1]. There are a variety of etiological factors for CKD, such as diabetes and hypertension, that contribute to the common pathological alteration, renal fibrosis, that results in renal function impairment [2]. Unfortunately, limited therapeutic options are available in clinical practice for patients with renal fibrosis [3]. Therefore, dissecting the mechanisms underlying renal fibrosis is imperative for the development of effective therapies for CKD prevention and reversal.

The weighted gene co-expression network analysis has revealed that prominin 1 (PROM1) is one of the hub signatures in renal fibrosis, and its significant downregulation has been detected in CKD [4,5]. The transmembrane protein PROM1 is a glycoprotein consisting of 865 amino acids [6]. Hori *et al.* [7] have demonstrated that PROM1 is implicated in membrane morphology, as evidenced by PROM1 overexpression leading to multiple, long, cholesterol-enriched fibres in human retinal pigment epithelial cells. On the other hand, PROM1 was reported to protect against liver fibrosis *via* negative regulation of transforming growth factor-β (TGF-β) signaling [8]. However, whether PROM1 plays a role in renal fibrosis remains unclear.

Journal of
BIOLOGICAL REGULATORS
and Homeostatic Agents

It has been shown that PROM1 regulates glycolysis by suppressing the activation of mammalian target of rapamycin (mTOR) complex 1 (mTORC1), a mediator of renal fibrosis [9,10]. mTORC1, consisting of mTOR, the regulatory-associated protein of mTOR (Raptor), and mLST8, regulates cell growth by phosphorylating downstream targets, including p70 S6 kinase (S6K) [11]. Furthermore, mTORC1 inhibition induces a dramatic decrease in 6-phosphofructo-2-kinase/fructose-2,6-bisphosphatase 3 (PFKFB3) [12]. Of note, PFKFB3, a key kinase in glycolysis, is the preferred energy source for fibroblasts in fibrotic diseases [13]. Studies have found that PFKFB3-mediated glycolysis in endothelial cells and fibroblasts participates in the process of renal fibrosis [14,15]. Although there are no studies that implicate PFKFB3-mediated glycolysis in renal fibrosis in renal tubular epithelial cells, we discovered that PFKFB3 is one of the differentially expressed genes in renal fibrosis using the GSE66494 database (https://www.ncbi.nlm.nih.gov/geo/query/acc.cgi?acc=GSE66494). Thus, we hypothesized that PFKFB3 plays a role in renal fibrosis through promotion of glycolysis in renal tubular epithelial cells.

In the current study, using a renal fibrosis mouse model induced *via* unilateral ureteric obstruction (UUO), and a cell model with TGF-β-stimulated human renal cortical proximal convoluted tubular epithelial cell line, HK-2, we found that PROM1 was lowly expressed in renal fibrosis, and PROM1 upregulation inhibited PFKFB3-driven glycolysis to ameliorate renal fibrosis by blocking mTORC1 pathway.

Objects and Methods

Animals

Male C57BL/6J mice (8–10 weeks old, 20–22 g, n = 36) provided by Hangzhou Medical College (Zhejiang, China) were raised under a specific pathogen-free environment (22–24 °C, 50–60% humidity, a 12-h light/dark cycle), with 2 or 3 mice in a cage. All mice had free access to food and water. All animal studies followed the recommendations in the guidelines of the China Council on Animal Care and Use Health. All operations on mice were approved by the Institutional Animal Care and Use Committee of Zhejiang Center of Laboratory Animals (No. ZJCLA-IACUC-20010529).

Induction of UUO Model

After a week of acclimation, twelve C57BL/6J mice were randomly selected and divided into Sham and Model groups (n = 6/group). Mice were anesthetized with 1.5% isoflurane (R510-22-16, PHR2874, Sigma-Aldrich, St. Louis, MI, USA) by inhalation before UUO modeling or sham operation, as described in a previous study [16]. To induce UUO models, left proximal ureters of mice were ligated with 4-0 silk at two points, and an incision was created between the two ligation locations. The ureters of the Sham group were made visible without ligation. On the 14th day following the procedure, the mice were sacrificed by cervical dislocation under anesthesia using 150 mg/kg of sodium pentobarbital (intraperitoneal injection, P3761, Haoran Biological Technology, Shanghai, China). Kidney tissues were later removed and preserved at –80 °C.

Quantitative Real-Time Reverse Transcription Polymerase Chain Reaction (qRT-PCR)

Total RNA of kidney tissues was extracted with a TRIzol™ Plus RNA Purification Kit (12183555, Thermo Scientific, Waltham, MA, USA), and then synthesized into first-strand complementary DNA (cDNA) using a SuperScript™ VILO™ cDNA Synthesis Kit (11754050, Thermo Scientific, Waltham, MA, USA). QRT-PCR was carried out in a reaction system, consisting of cDNA, specific primers of *PROM1* (forward: 5′-CTCATGGCTGGGGTTGGATT-3′; reverse: 5′-TGAGCAGATAGGGAGTGTCCA-3′) and β-actin (forward: 5′-ATATCGCTGCGCTGGTCGTC-3′; reverse: 5′-AGGATGGCGTGAGGGAGAGC-3′), and Fast SYBR™ Green Master Mix (4385612, Thermo Scientific, Waltham, MA, USA) in a QuantStudio™ 7 Pro real-time PCR instrument (A43165, Thermo Scientific, Waltham, MA, USA), with the following conditions: 95 °C for 20 s, and 40 cycles at 95 °C for 3 s and 60 °C for 30 s. Data were processed using the $2^{-\Delta\Delta Ct}$ method [17], with β-actin as the internal control.

PROM1 Overexpression in Vivo

The pHAGE-*PROM1* vector and empty vector as negative control (NC, 166467) were obtained from Addgene (Cambridge, MA, USA). The 24 mice were assigned into Sham, Model, Model+NC, and Model+PROM1 groups (6 mice/group), and were subjected to sham or UUO operation as described above. After surgeries, mice in the Model+NC and Model+PROM1 groups were separately injected with 50 µL transfection solution containing 15 µg empty vector and pHAGE-*PROM1* vector *via* tail vein for 6 weeks, once a week [18]. Finally, detached kidney tissues were either preserved at –80 °C or fixed in 4% paraformaldehyde solution (abs9179, Absin, Shanghai, China).

Tissue Staining

After 48-h fixation, kidney tissues were dehydrated in alcohol (51976, Sigma-Aldrich, St. Louis, MI, USA) and permeabilized in xylene (XX0060, Sigma-Aldrich, St. Louis, MI, USA). Then, 6-µm tissue sections were made following paraffin embedment. For staining, sections were deparaffinized in xylene and rehydrated with gradient ethanol.

To observe pathological changes, hematoxylin (H3136, Sigma-Aldrich, St. Louis, MI, USA) and eosin (861006, Sigma-Aldrich, St. Louis, MI, USA) (H&E) staining was used to dye sections for 5 min and 3 min, respectively, at room temperature. The assessment of

interstitial fibrosis and tubular damage was performed by section staining with Masson's Trichrome Stain Kit (G1340, Solarbio, Beijing, China) and Sirius red (30 min, S8060, Solarbio, Beijing, China), respectively. Finally, after being sealed with neutral gum, the stained sections were observed under the BX53M optical microscope (×100 magnification, OLYMPUS, Tokyo, Japan).

Next, immunohistochemistry staining was performed to detect the expression of PFKFB3 in kidney tissues. In brief, sections were maintained in phosphate-buffered saline (PBS, abs962, Absin, Shanghai, China) supplemented with TritonX-100 (A1009, Applygen, Beijing, China) and 30% H_2O_2 (323381, Sigma-Aldrich, St. Louis, MI, USA) for 30 min against the light at room temperature. Afterwards, antigen repair buffer (B1055, Applygen, Beijing, China) and 5% goat serum (C1771, Applygen, Beijing, China) were incubated with sections at 37 °C for 20 min or at room temperature for 30 min. The sections were successively cultured with anti-PFKFB3 antibody (MA5-32766, Thermo Scientific, Waltham, MA, USA) overnight at 4 °C and horseradish peroxidase (HRP)-conjugated Goat anti-Rabbit IgG (31460, Thermo Scientific, Waltham, MA, USA) at 37 °C for 30 min. Finally, DAB Substrate Solution (B1072, Applygen, Beijing, China) was applied for color development, followed by re-staining with hematoxylin, alcohol dehydration, xylene permeabilization, and neutral gum sealing. A BX53M optical microscope was utilized to observe sections at ×100 magnification.

Cell Culture and Transfection

HK-2 (AW-CELLS-H0142, AnWei-sci, Shanghai, China) cells were grown in serum-free medium for keratinocytes (AW-M014, AnWei-sci, Shanghai, China) containing 10% fetal bovine serum (FBS, AW-FBS-001, AnWei-sci, Shanghai, China). The cells were incubated in 96-well plates (1×10^4 cells/well) in a 37 °C incubator under 5% CO_2. All cells were routinely subjected to STR identification and mycoplasma contamination tests, and were confirmed to be mycoplasma-free.

For cell transfection, PROM1 overexpression plasmid was synthesized using pcDNA3.1 vectors (VT1001), with empty vectors as NC, and both vectors were purchased from YouBio (Changsha, China). Cells were grown to 70–90% confluency, before addition of liposome complexes of PROM1 overexpression vectors/empty vectors prepared using Lipofectamine 3000 Reagent (L3000001, Thermo Scientific, Waltham, MA, USA) for 48 h at 37 °C. The transfection efficiency was measured through western blot.

Cell Treatment

Subsequently, HK-2 cells were exposed to various treatments to investigate the effect of PROM1 on TGF-β-induced cells. First, cells in Control, TGF-β, TGF-β+NC, and TGF-β+PROM1 groups were seeded in 6-well plates containing complete medium overnight, and were starved in serum-free medium for 12 h. Cells in the latter three groups were incubated with 20 ng/mL human recombinant TGF-β (GF346, Sigma-Aldrich, St. Louis, MI, USA) in complete medium at 37 °C for 24 h [19], followed by observation of cell morphology using a BX53M microscope at ×200 magnification.

For treatment with mTOR activator MHY1485 (SML0810, Sigma-Aldrich, St. Louis, MI, USA), HK-2 cells were distributed into NC (control HK-2 cells treated with TGF-β), PROM1 (PROM1-overexpressing HK-2 cells treated with TGF-β), MHY1485 (normal HK-2 cells treated with 2 μM MHY1485 and TGF-β), and PROM1+MHY1485 groups (PROM1-overexpressing HK-2 cells treated with 2 μM MHY1485 and TGF-β). Specifically, MHY1485 was dissolved in dimethyl sulfoxide (abs9184, Absin, Shanghai, China) and diluted in complete medium to treat cells for 6 h before TGF-β treatment [20].

Lactate Assay

A Lactate Assay Kit (MAK064, Sigma-Aldrich, St. Louis, MI, USA) was utilized to detect lactate content in the supernatant of culture medium. In brief, 50 μL/well samples and different concentrations of standards were added into 96-well plates as per well-setting positions, and incubated with 50 μL prepared Master Reaction Mix for 30 min at room temperature in the dark. The absorbance at 570 nm was measured in Multiskan™ FC Microplate Photometer (51119180ET, Thermo Scientific, Waltham, MA, USA).

Extracellular Acidification Rate (ECAR)

ECAR measurement was achieved with the Seahorse XF Glycolysis Stress Test Kit (103020-100, Agilent, Santa Clara, CA, USA) and Seahorse XFe24 Analyzer (Agilent, Santa Clara, CA, USA) as previously described [21]. In detail, the number of transfected cells was counted. Glucose, oligomycin (an inhibitor of oxidative phosphorylation) and 2-DG (a glycolytic inhibitor) were added into each well at the designated time intervals. Seahorse XFp Wave software (Agilent, Santa Clara, CA, USA) was used to analyze the data that were expressed as mpH/min. After cell digestion with Trypsin (P4201, Beyotime, Shanghai, China) in each well and cell quantification with a cell counting chamber, the results were normalized to the number of cells in each well.

Western Blot

Kidney tissues and HK-2 cells were treated with RIPA Buffer (R0010, Solarbio, Beijing, China) supplemented with mixture of protease and phosphatase inhibitor (P1261, Solarbio, Beijing, China) to extract proteins. Following 5-min boiling water bath, protein concentration was determined with BCA Protein Assay Kit (PC0020, Solarbio, Beijing, China) and protein separation was completed by sodium dodecyl sulfate polyacrylamide gel electrophoresis in NuPAGE™ 4–12%, Bis-Tris (NP0321BOX, Thermo Scientific, Waltham, MA, USA). After being loaded with separated proteins, polyvinylidene fluoride (PVDF) mem-

Journal of
BIOLOGICAL REGULATORS
and Homeostatic Agents

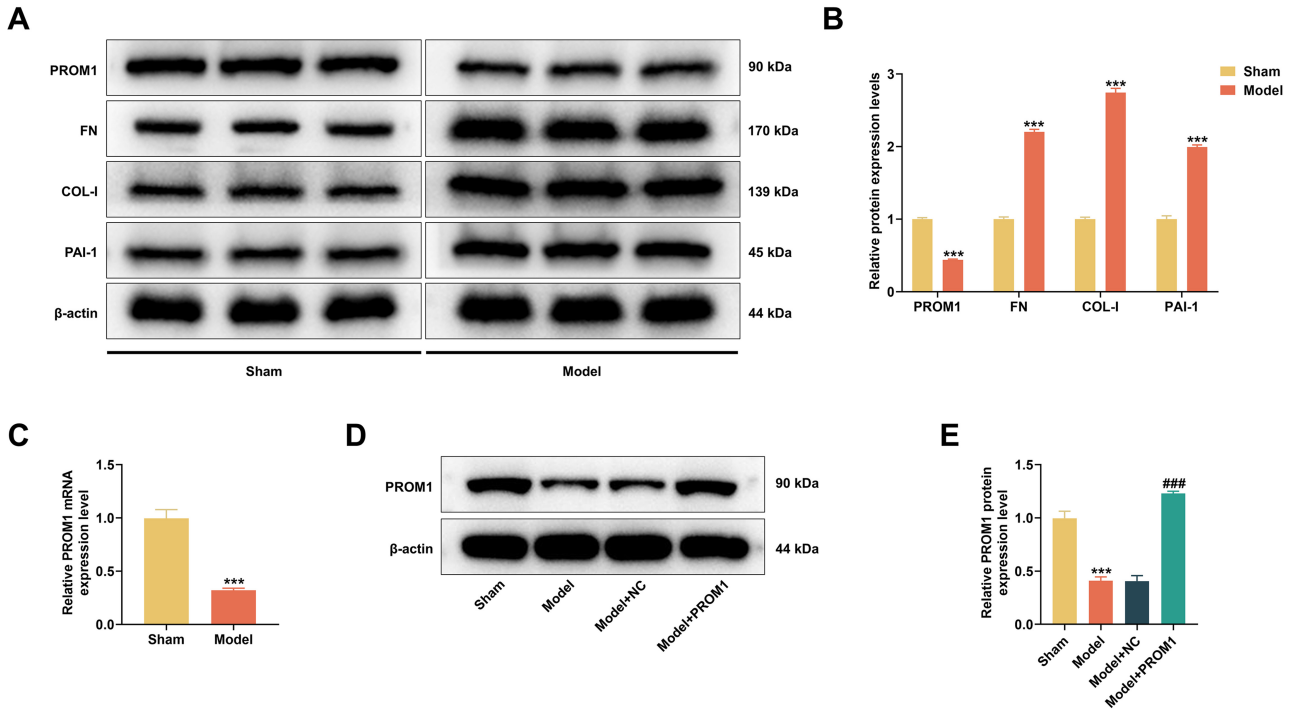

Fig. 1. Expression of PROM1 and fibrosis-related proteins in kidneys of UUO mice. (A,B) Expression of PROM1 and fibrosis-related proteins (FN, COL-I, and PAI-1) was measured by western blot in kidney tissues of mice in Sham and Model groups. (C) The mRNA expression of *PROM1* was tested by qRT-PCR in kidney tissues of mice in Sham and Model groups. (D,E) Vectors of pHAGE-*PROM1* or empty vectors as negative control were injected into model mice *via* tail vein (Model+PROM1 and Model+NC groups), or not (Model group), with Sham group as the blank control, and western blot data displayed the protein expression of PROM1. β-actin was used as an internal reference. $^{***}p < 0.001$ *vs.* Sham; $^{\#\#\#}p < 0.001$ *vs.* Model+NC. PROM1, prominin 1; UUO, unilateral ureteric obstruction; FN, fibronectin; COL-I, type I collagen; PAI-1, plasminogen activator inhibitor-1; qRT-PCR, quantitative real-time reverse transcription polymerase chain reaction; NC, negative control.

branes (YA1701, Solarbio, Beijing, China) were blocked with Blocking Buffer (37581, Thermo Scientific, Waltham, MA, USA) for 1 h at room temperature, probed first with primary antibodies at 4 °C overnight, and then incubated with secondary antibodies for 1 h at room temperature. Following the BeyoECL Plus (P0018S, Beyotime, Shanghai, China) treatment, the band signals were analyzed on 5200 imaging system (Tanon, Shanghai, China). Data analysis was performed using Image J software (1.52s version, National Institutes of Health, Bethesda, MD, USA), with β-actin as an internal reference.

Antibodies obtained from Abcam (Cambridge, UK) were as follows: PROM1 (ab284389, 90/97 kDa, 1:1000), type I collagen (COL-I; ab260043, 120/139 kDa, 1:1000), plasminogen activator inhibitor-1 (PAI-1; ab222754, 44/45 kDa, 1:1000), Raptor (ab40768, 125/140 kDa, 1:1000), Rictor (ab105469, 192 kDa, 1:1000), hexokinase 2 (HK2; ab209847, 102/112 kDa, 1:1000), PFKFB3 (ab181861, 58/62 kDa, 1:1000), β-actin (ab8226, 44 kDa, 1:1000), HRP-coupled Goat anti-Rabbit IgG (ab205718, 1:2000) and HRP-coupled Goat anti-Mouse IgG (ab205719, 1:2000). In addition, phosphorylated S6K (p-S6; 4858, 32 kDa, 1:2000) and mTOR (2972, 180/200 kDa, 1:1000) were procured from Cell Signaling Technology (Beverly, MA, USA), and fibronectin (FN; WL03677, 170/200/250 kDa, 1:1000) was obtained from Wanleibio (Shenyang, China).

Statistical Analysis

All data in this study were obtained from three independent assays, expressed as mean ± standard deviation, and analyzed by GraphPad Prism 8 (GraphPad, Inc., La Jolla, CA, USA). Data in Fig. 1A–C were analyzed using independent samples *t*-tests. Differences among multiple groups in Fig. 5B and Fig. 6N were analyzed by either one-way or two-way analysis of variance. p-value < 0.05 was considered statistically significant.

Results

PROM1 was Lowly Expressed in Renal Fibrosis of UUO Mice

To induce renal fibrosis, we performed a UUO operation on mice. Western blot results demonstrated that expressions of fibrosis-related proteins FN, COL-I, and PAI-1 [22] were increased in kidneys of UUO mice as compared with

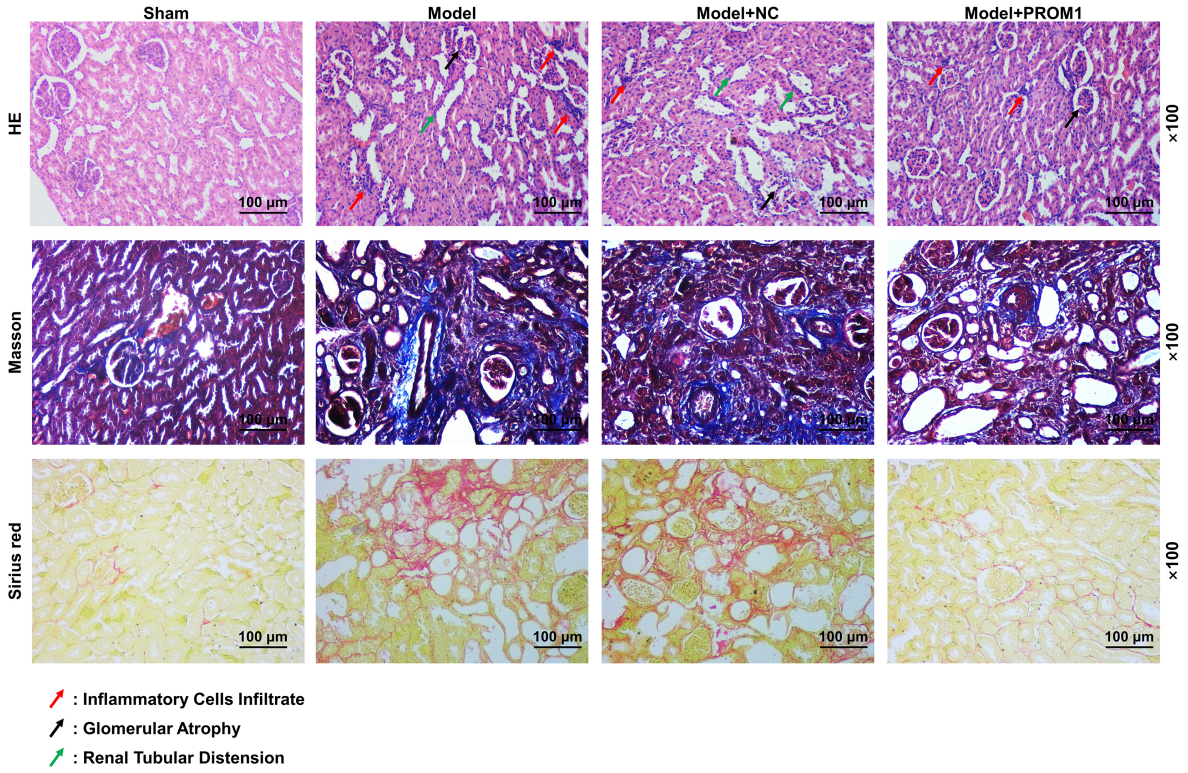

Fig. 2. Effect of PROM1 overexpression on renal fibrosis of UUO mice. Tissue staining (H&E, Masson, and Sirius red) of kidneys from sham and UUO mice with/without PROM1 overexpression, at the magnification of ×100 and scale of 100 μm. H&E, hematoxylin and eosin; NC, negative control.

sham mice (Fig. 1A,B, $p < 0.001$). In addition, the protein expression of PROM1 was lower in kidneys of UUO mice than sham mice (Fig. 1A,B, $p < 0.001$). PROM1 mRNA expression in kidneys of UUO mice was also lower than that of sham mice (Fig. 1C, $p < 0.001$).

PROM1 Overexpression Inhibited Renal Fibrosis, the mTORC1 Pathway, and PFKFB3-Driven Glycolysis in UUO Mice

To explore the role of PROM1 in renal fibrosis, PROM1 was overexpressed in UUO mice *via* injection with pHAGE-*PROM1* vectors (Fig. 1D,E, $p < 0.001$). As illustrated in Fig. 2, severe tubular dilatation and atrophy, inflammatory cell infiltration, and collagen and fibrin formation in the tubulointerstitium were observed in the Model group. The renal tissue shape and pathological change in Model+NC group were comparable to those in Model group. By comparison with Model+NC group, Model+PROM1 group showed significantly reduced renal fibrotic lesions (Fig. 2), suggesting the alleviation of PROM1 overexpression on renal fibrosis. According to molecular detection results, the upregulation of FN, COL-I, and PAI-1 in kidneys of UUO mice was suppressed following PROM1 overexpression, as evidenced by their reduced expression in the Model+PROM1 group compared with the Model+NC group (Fig. 3A–D, $p < 0.05$).

Upregulation of mTOR, Raptor, Rictor, and p-S6 was detected in kidneys of UUO mice (Fig. 3E–I, $p < 0.01$), suggesting that the mTORC1 pathway may be activated in renal fibrosis [23]. Comparison of Model+PROM1 and Model+NC groups indicated that PROM1 overexpression inhibited the mTORC1 pathway by blocking expressions of mTOR, Raptor, Rictor, and p-S6 (Fig. 3E–I, $p < 0.05$). Furthermore, expressions of glycolysis-related proteins HK2 and PFKFB3 [24] were higher in kidneys of UUO mice than sham mice (Fig. 3E,J,K, $p < 0.001$), and these increases were counteracted following PROM1 overexpression in UUO mice (Fig. 3E,J,K, $p < 0.01$). As shown in Fig. 3L, immunohistochemistry staining revealed that PFKFB3 expression was increased in kidneys of UUO mice; however, PROM1 overexpression decreased PFKFB3 expression in UUO mice. These findings demonstrated that PROM1 overexpression suppressed the mTORC1 pathway and PFKFB3-driven glycolysis in kidneys of UUO mice.

PROM1 Overexpression Relieved Fibrosis and PFKFB3-Driven Glycolysis, and Inhibited the mTORC1 Pathway in TGF-β-Induced HK-2 Cells

To elucidate the mechanism of PROM1 regulation of renal fibrosis, we treated HK-2 cells with 20 ng/mL human recombinant TGF-β to induce fibrosis. Following transfection of overexpression vectors, PROM1 was overexpressed

Journal of
BIOLOGICAL REGULATORS
and Homeostatic Agents

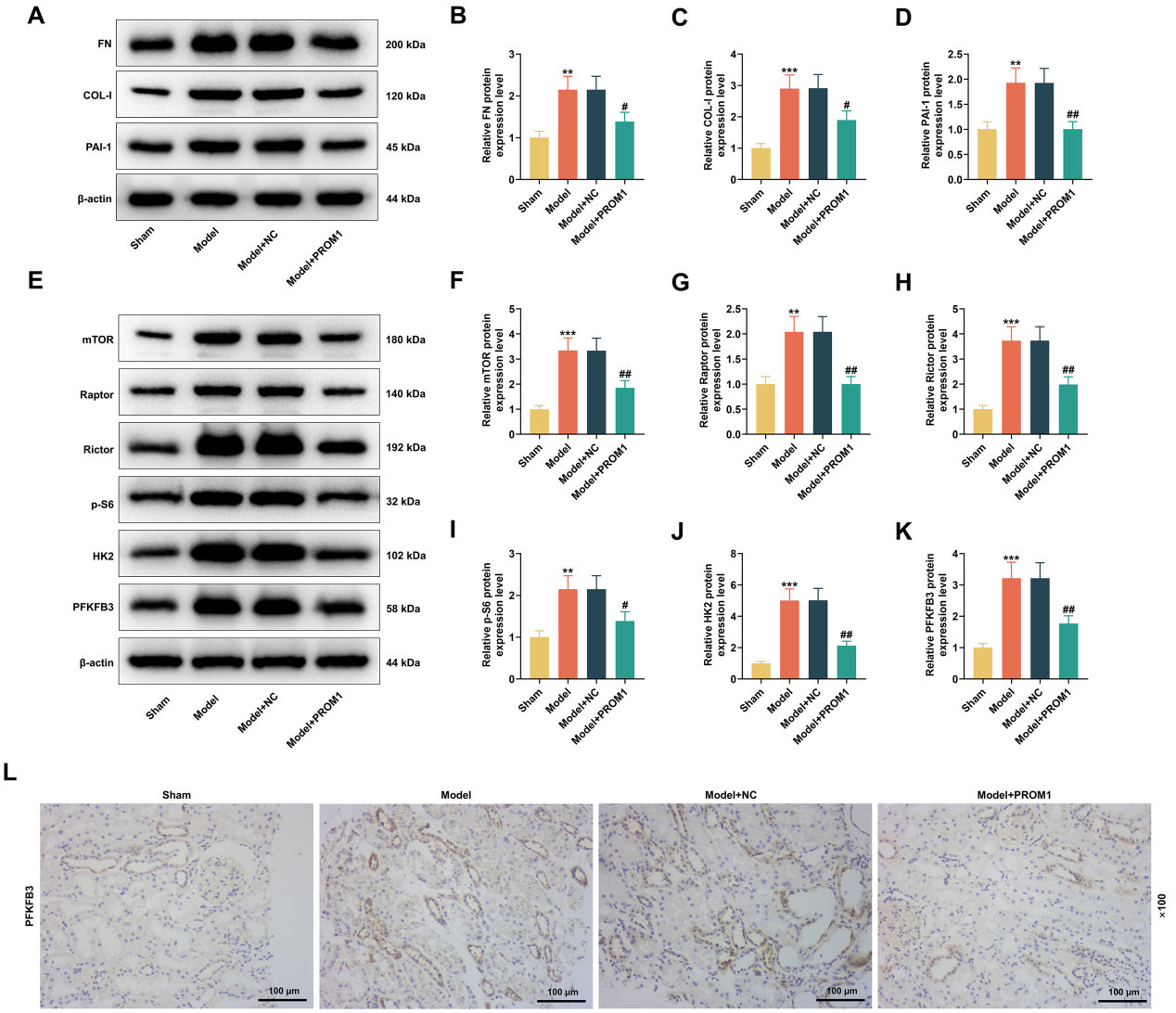

Fig. 3. Effect of PROM1 overexpression on protein expression related to fibrosis, the mTORC1 pathway, and glycolysis in kidneys of UUO mice. (A–K) Western blot data displayed protein expression related to fibrosis (FN, COL-I, PAI-1; A–D), mTORC1 pathway (mTOR, Raptor, Rictor, and p-S6; E–I), and glycolysis (HK2 and PFKFB3; E,J,K) in kidney tissues from sham and UUO mice in the presence or absence of PROM1 overexpression, with β-actin as an internal reference. (L) The location of PFKFB3 in immunohistochemistry staining of kidney tissues from sham and UUO mice with/without PROM1 overexpression, at the magnification of $\times 100$ and scale of 100 μm. $^{**}p < 0.01$, $^{***}p < 0.001$ *vs.* Sham; $^{\#}p < 0.05$, $^{\#\#}p < 0.01$ *vs.* Model+NC. mTOR, mammalian target of rapamycin; mTORC1, mTOR complex 1; Rictor, RPTOR independent companion of MTOR complex 2; p-S6, phosphorylated S6 ribosomal protein; HK2, hexokinase 2; PFKFB3, 6-phosphofructo-2-kinase/fructose-2,6-bisphosphatase 3; FN, fibronectin; COL-I, type I collagen; PAI-1, plasminogen activator inhibitor-1.

in HK-2 cells (Fig. 4A, $p < 0.001$). As shown in Fig. 4B, control cells had fusiform morphology, whereas TGF-β-treated cells showed fibroblast-like morphology, which was later relieved following PROM1 overexpression.

HK2 and PFKFB3 were highly expressed in TGF-β-induced HK-2 cells compared to control cells (Fig. 4C–E, $p < 0.001$), and this effect was reversed following PROM1 overexpression (Fig. 4C–E, $p < 0.01$). Lactate content in the supernatant of culture medium and ECAR of TGF-β-induced HK-2 cells reflected the glycolysis level [25]. We found that TGF-β stimulation led to more accumulation of lactate, a producer of glycolysis (Fig. 5A, $p < 0.001$), and a significant increase of ECAR, an indicator of glycolysis (Fig. 5B,C, $p < 0.001$). These effects were reversed by PROM1 overexpression by decreasing lactate content in cell supernatant (Fig. 5A, $p < 0.01$) and ECAR-indicated glycolysis (Fig. 5B,C, $p < 0.01$). Moreover, upregulation of FN, COL-I, and PAI-1 was observed in TGF-β-induced HK-2 cells (Fig. 5D–G, $p < 0.01$), and their downregulation was detected after treatment of TGF-β and PROM1 overex-

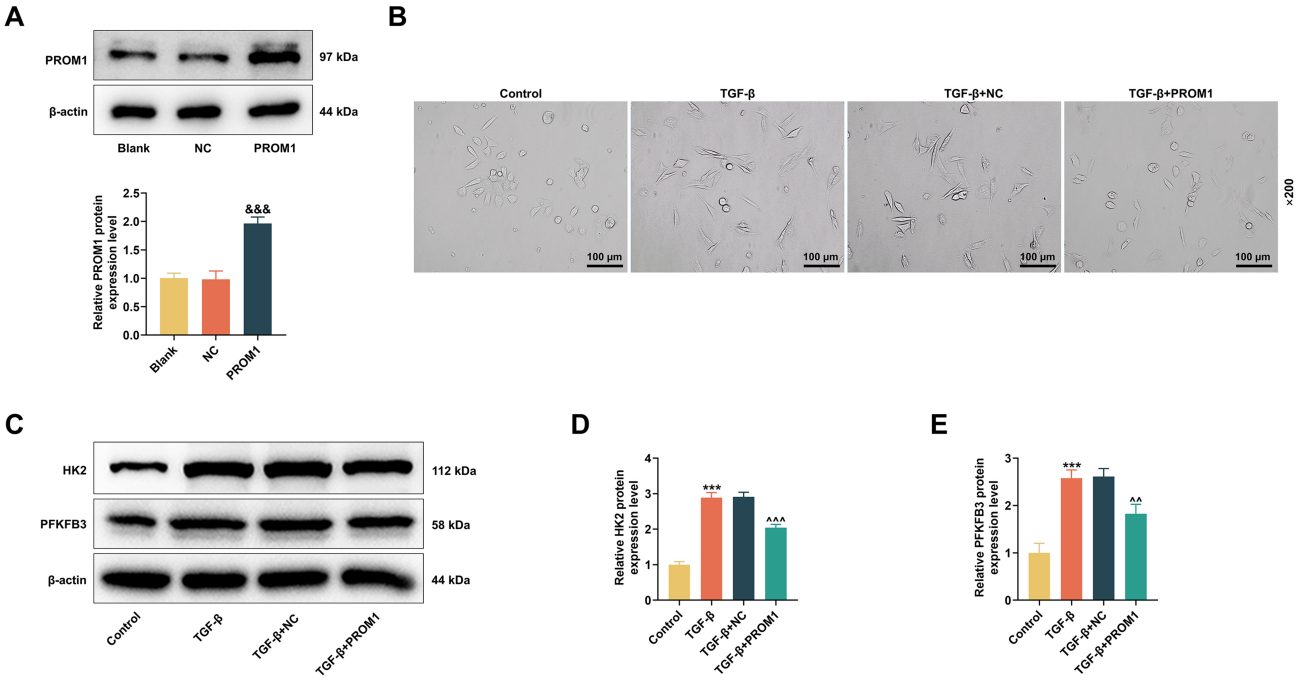

Fig. 4. Effects of PROM1 overexpression on fibrosis and glycolysis-related protein expression in TGF-β-induced HK-2 cells. (A) PROM1 protein expression was quantified by western blot in HK-2 cells transfected with/without PROM1 overexpression vectors or empty vectors. (B) Representative images of HK-2 cells with/without TGF-β treatment and PROM1 overexpression, at the magnification of $\times$200 and scale of 100 μm. (C–E) Expression of glycolysis-related proteins (HK2 and PFKFB3) in HK-2 cells with/without TGF-β treatment and PROM1 overexpression. β-actin was used as an internal reference. $^{\&\&\&}p < 0.001$ *vs.* NC; $^{***}p < 0.001$ *vs.* Control; $^{\wedge\wedge}p < 0.01$, $^{\wedge\wedge\wedge}p < 0.001$ *vs.* TGF-β+NC. TGF-β, transforming growth factor-β.

pression vector (Fig. 5D–G, $p < 0.05$). In addition, TGF-β treatment resulted in increased expressions of mTOR, Raptor, Rictor, and p-S6 in HK-2 cells (Fig. 5D,H–K, $p < 0.01$), but PROM1 overexpression downregulated these proteins in TGF-β-induced cells (Fig. 5D,H–K, $p < 0.05$). These results verified that PROM1 overexpression relieved fibrosis and PFKFB3-driven glycolysis, and inhibited mTORC1 pathway in TGF-β-induced HK-2 cells.

mTORC1 Activator Reversed the Inhibitory Effect of PROM1 Overexpression on Fibrosis in Vitro by Regulating the mTORC1 Pathway and PFKFB3-Driven Glycolysis

We initially demonstrated the inactivation of the mTORC1 pathway by PROM1 overexpression in Western blot, which was further confirmed *via* cell treatment with MHY1485, a mTORC1 activator. In TGF-β-induced cells, MHY1485 led to the upregulation of mTORC1 pathway-related proteins (mTOR, Raptor, Rictor, and p-S6) (Fig. 6A–E, $p < 0.001$), fibrosis-associated proteins (FN, COL-I, and PAI-1) (Fig. 6F–I, $p < 0.001$), and glycolysis-related proteins (HK2 and PFKFB3) (Fig. 6J–L, $p < 0.001$), which was later suppressed by PROM1 overexpression (Fig. 6A–L, $p < 0.001$). Moreover, MHY1485 counteracted the downregulation of these proteins by PROM1 overexpression in TGF-β-induced cells (Fig. 6A–L, $p < 0.01$). As for glycolysis at the cellular level, lactate accumulation and ECAR were found to be higher in the MHY1485 group than in the NC group (Fig. 6M–O, $p < 0.01$), whereas these two indicators were diminished in the PROM1+MHY1485 group compared to MHY1485 group (Fig. 6M–O, $p < 0.01$). Also, lactate accumulation was increased in PROM1+MHY1485 group as compared with PROM1 group (Fig. 6M, $p < 0.01$).

Discussion

Fibrotic matrix formation is linked to the tissue repair process in the early phases of damage. But if tissue damage persists, unchecked inflammatory reactions and fibrotic matrix deposition occur, resulting in compromised kidney structure and, ultimately, CKD [26]. Accumulating evidence has confirmed the association between PROM1 and fibrosis in biliary atresia [27,28]. However, existing reports have not clarified whether PROM1 participates in the renal fibrosis of CKD. Here, we demonstrated that PROM1 was lowly expressed in renal fibrosis in UUO mice and that PROM1 overexpression played a relieving role in fibrosis both in UUO mice and in TGF-β-induced HK-2 cells. Additionally, we found that PROM1 might function by inactivating mTORC1 pathway to resist PFKFB3-driven glycolysis.

Journal of
BIOLOGICAL REGULATORS
and Homeostatic Agents

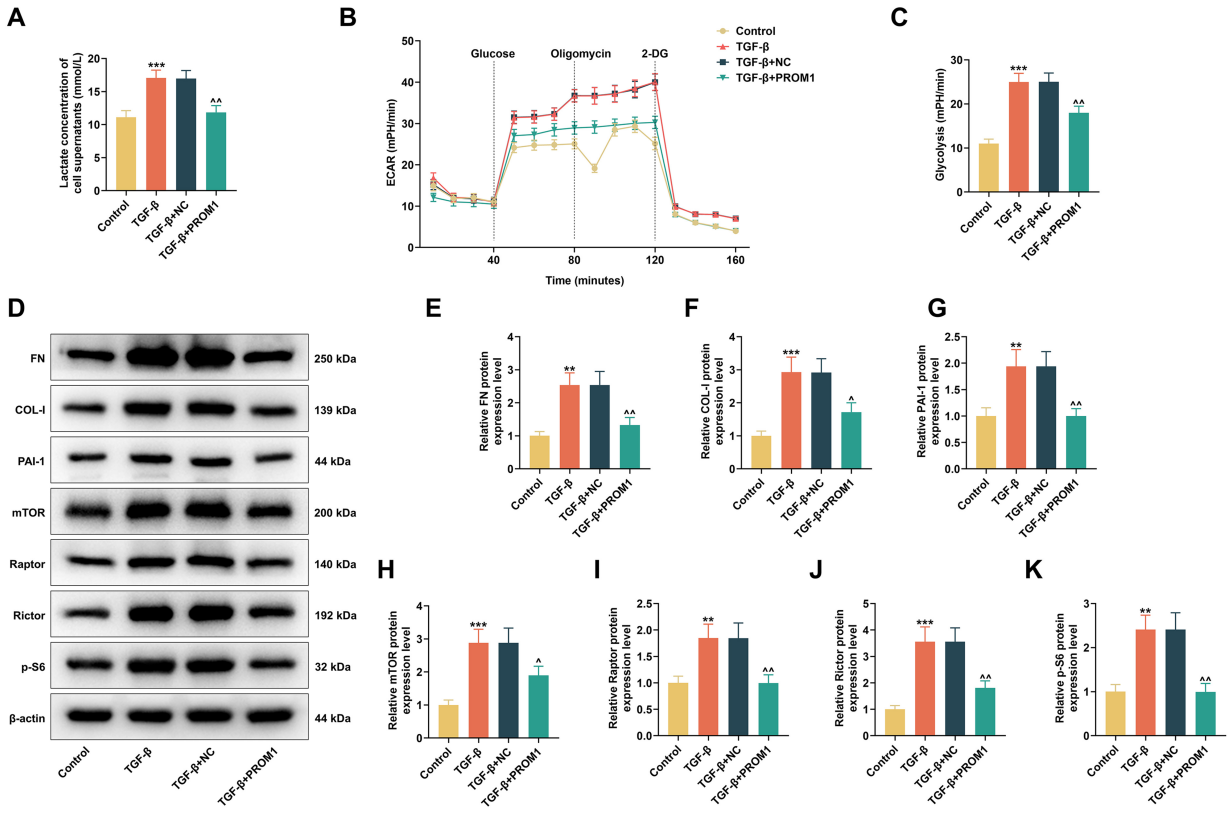

Fig. 5. Effects of PROM1 overexpression on glycolysis and expressions of fibrosis/mTORC1 pathway-related proteins in TGF-β-induced HK-2 cells. (A) Lactate content in the culture medium of supernatant of HK-2 cells with/without TGF-β treatment and PROM1 overexpression. (B,C) ECAR of HK-2 cells with/without TGF-β treatment and PROM1 overexpression was determined by Seahorse XFe24 Analyzer after glucose, oligomycin (an inhibitor of oxidative phosphorylation), and 2-DG (a glycolytic inhibitor) were added at the designated time intervals. (D–K) Western blot data for expression of fibrosis-related proteins (FN, COL-I, PAI-1; D–G) and mTORC1 pathway-related proteins (mTOR, Raptor, Rictor, and p-S6; D,H–K) in HK-2 cells with/without TGF-β treatment and PROM1 overexpression. β-actin was used as an internal reference. $^{**}p < 0.01$, $^{***}p < 0.001$ *vs.* Control; $^{\wedge}p < 0.05$, $^{\wedge\wedge}p < 0.01$ *vs.* TGF-β+NC. ECAR, extracellular acidification rate.

The characteristic feature of fibrosis in kidney tubules is the excessive accumulation of extracellular matrix (ECM) caused by the activation and proliferation of interstitial fibroblasts [29]. In fibrogenesis of renal fibroblasts, TGF-β is responsible for the transformation from myofibroblast to interstitial fibroblast, and induces expressions of FN, COL-I, and PAI-1, leading to ECM deposition and impaired degradation [30,31]. In this study, we observed that TGF-β promoted fibroid changes and expressions of FN, COL-I, and PAI-1 in HK-2 cells *in vitro*. In addition, the same increases were identified in kidneys of UUO mice, accompanied by severe tubular dilatation and atrophy, and inflammatory cell infiltration in the renal tubular interstitium. Importantly, these fibrotic features were improved after PROM1 overexpression in UUO mice and HK-2 cells, consistent with the protective role of PROM1 against liver fibrosis [8]. However, previous studies have also reported that PROM1 promotes biliary atresia-related fibrosis [27,28], suggesting functional heterogeneity of PROM1.

In recent years, the relation between aerobic glycolysis and renal fibrosis has attracted increasing attention. Numerous studies revealed that enhanced aerobic glycolysis provides energy for fibroblast-myofibroblast transdifferentiation fibrosis, and is associated with inflammation, resulting in renal fibrosis, and inhibition of glycolysis contributes to attenuation of renal fibrosis [32–35]. As a key glycolysis activator, PFKFB3 is significantly upregulated in kidneys of UUO mice, and decreased fibrosis has been detected in injured kidneys of PFKFB3-deficient UUO mice. The study by Yang *et al.* [36] reported that the PFKFB3-driven glycolysis in myeloid cells also takes part in renal fibrosis of UUO mice. Another crucial rate-limiting enzyme related to the glycolytic pathway, HK2, is involved in metabolic dysregulation during fibrogenesis [37]. Here, we identified upregulation of HK2 and PFKFB3 in fibrotic kidneys and cells, and increased lactate content as well as ECAR in TGF-β-treated cells. Of note, PROM1 overexpression attenuated glycolysis *in vivo* and *in vitro*, implying that PROM1 overexpression alleviated renal fibro-

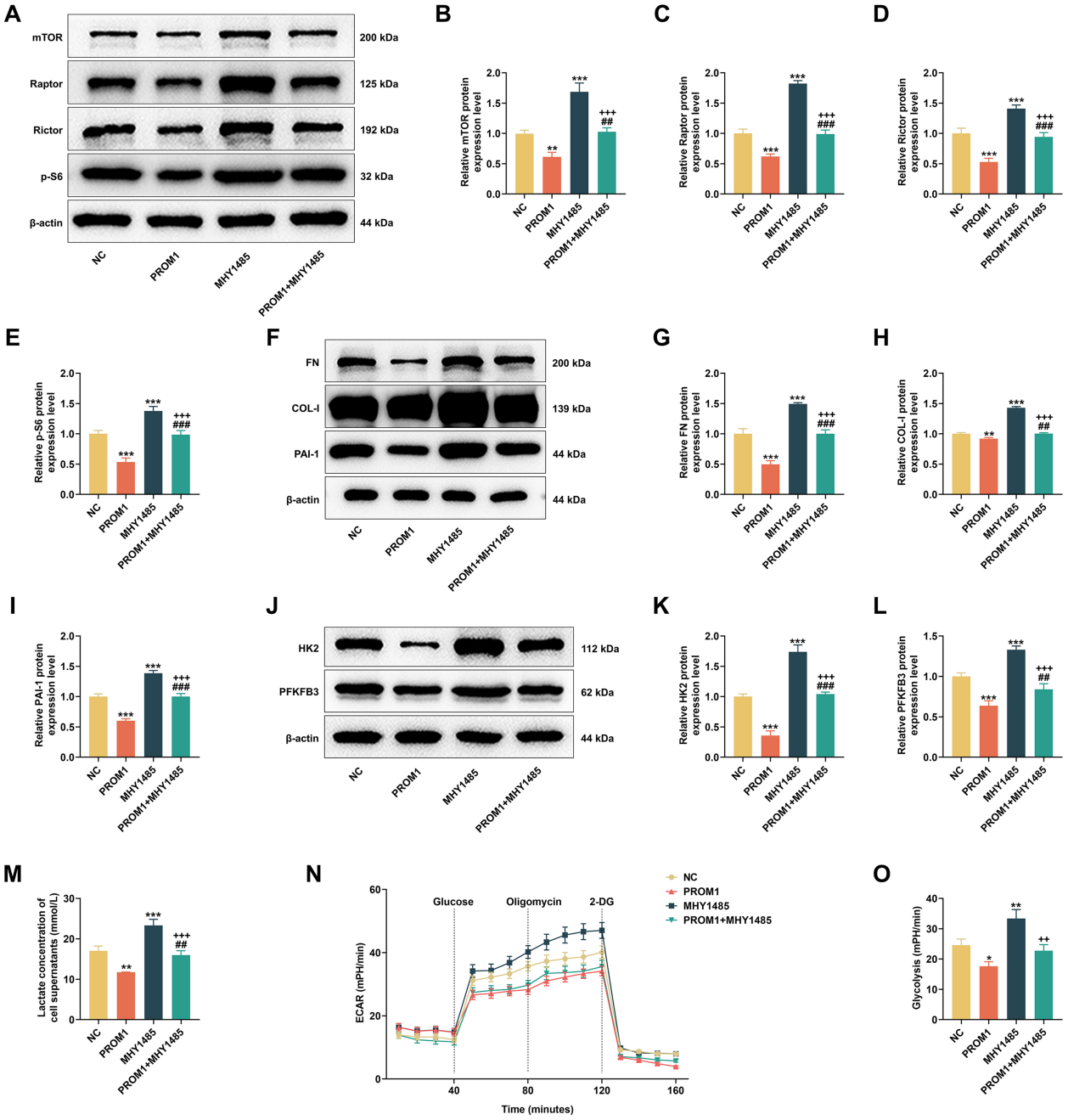

Fig. 6. Effects of mTORC1 activator on PROM1 overexpression-regulated mTORC1 pathway, fibrosis, and PFKFB3-driven glycolysis. (A–L) Western blot data revealed expressions of mTORC1 pathway-related proteins (mTOR, Raptor, Rictor, and p-S6; A–E), fibrosis-related proteins (FN, COL-I, and PAI-1; F–I), and glycolysis-related proteins (HK2 and PFKFB3; J–L) in TGF-β-stimulated HK-2 cells in the presence or absence of MHY1485 (mTORC1 activator) treatment and/or PROM1 overexpression (NC, PROM1, MHY1485, and PROM1+MHY1485 groups), with β-actin as an internal reference. (M) Lactate content in the culture medium of supernatant of TGF-β-stimulated HK-2 cells with/without MHY1485 treatment and PROM1 overexpression. (N,O) ECAR of TGF-β-stimulated HK-2 cells with/without MHY1485 treatment and PROM1 overexpression was determined with Seahorse XFe24 Analyzer after glucose, oligomycin, and 2-DG were added at the designated time intervals. $^{*}p < 0.05$, $^{**}p < 0.01$, $^{***}p < 0.001$ *vs.* NC; $^{++}p < 0.01$, $^{+++}p < 0.001$ *vs.* MHY1485; $^{\#\#}p < 0.01$, $^{\#\#\#}p < 0.001$ *vs.* PROM1.

sis through suppression of aerobic glycolysis. In addition, it has been reported that mTORC1 activation in renal proximal tubule cells induces tubulointerstitial fibrosis through regulation of glycolysis [9,38]. In the current study, mTORC1 pathway-related proteins were highly expressed in fibrotic kidneys and cells, whereas PROM1 overexpres-

Journal of
BIOLOGICAL REGULATORS
and Homeostatic Agents

sion caused inhibition of the mTORC1 pathway, which was reversed by mTORC1 activator. These findings indicated that PROM1 functions by inhibiting mTORC1, similar to a previous study [10]. Interestingly, Rictor, a component of mTORC2, was found to have the same expression changes as the mTORC1 pathway in this study. This suggests the possible involvement of mTORC2 in the mechanism of PROM1 regulating renal fibrosis. Based on this, further research is necessary.

Conclusion

To sum up, this study highlights the crucial role and potential mechanism of PROM1 upregulation in renal tubular epithelial cells, namely the protective effect against glycolysis-mediated kidney fibrosis. Our results indicate that targeting PROM1 is a promising new method for CKD prevention and treatment.

Availability of Data and Materials

The analyzed data sets generated during the study are available from the corresponding author on reasonable request.

Author Contributions

Substantial contributions to conception and design: TS, HY. Data acquisition, data analysis and interpretation: MC, CY. Drafting the article or critically revising it for important intellectual content: All authors. Final approval of the version to be published: All authors. Agreement to be accountable for all aspects of the work in ensuring that questions related to the accuracy or integrity of the work are appropriately investigated and resolved: All authors.

Ethics Approval and Consent to Participate

All animal studies followed the recommendations in the guidelines of the China Council on Animal Care and Use Health. All operations on mice were approved by the Institutional Animal Care and Use Committee of Zhejiang Center of Laboratory Animals (No. ZJCLA-IACUC-20010529).

Acknowledgment

Not applicable.

Funding

This research received no external funding.

Conflict of Interest

The authors declare no conflict of interest.

References

[1] Kovesdy CP. Epidemiology of chronic kidney disease: an update 2022. Kidney International Supplements. 2022; 12: 7–11.

[2] Prakoura N, Hadchouel J, Chatziantoniou C. Novel Targets for Therapy of Renal Fibrosis. The Journal of Histochemistry and Cytochemistry: Official Journal of the Histochemistry Society. 2019; 67: 701–715.

[3] Yamashita N, Kramann R. Mechanisms of kidney fibrosis and routes towards therapy. Trends in Endocrinology and Metabolism: TEM. 2024; 35: 31–48.

[4] Hu Z, Liu Y, Zhu Y, Cui H, Pan J. Identification of key biomarkers and immune infiltration in renal interstitial fibrosis. Annals of Translational Medicine. 2022; 10: 190.

[5] Guo Y, Ma J, Xiao L, Fang J, Li G, Zhang L, *et al*. Identification of key pathways and genes in different types of chronic kidney disease based on WGCNA. Molecular Medicine Reports. 2019; 20: 2245–2257.

[6] Ragi SD, Lima de Carvalho JR, Jr, Tanaka AJ, Park KS, Mahajan VB, Maumenee IH, *et al*. Compound heterozygous novel frameshift variants in the *PROM1* gene result in Leber congenital amaurosis. Cold Spring Harbor Molecular Case Studies. 2019; 5: a004481.

[7] Hori A, Nishide K, Yasukuni Y, Haga K, Kakuta W, Ishikawa Y, *et al*. Prominin-1 Modulates Rho/ROCK-Mediated Membrane Morphology and Calcium-Dependent Intracellular Chloride Flux. Scientific Reports. 2019; 9: 15911.

[8] Lee H, Yu DM, Bahn MS, Kwon YJ, Um MJ, Yoon SY, *et al*. Hepatocyte-specific Prominin-1 protects against liver injury-induced fibrosis by stabilizing SMAD7. Experimental & Molecular Medicine. 2022; 54: 1277–1289.

[9] Cao H, Luo J, Zhang Y, Mao X, Wen P, Ding H, *et al*. Tuberous sclerosis 1 (Tsc1) mediated mTORC1 activation promotes glycolysis in tubular epithelial cells in kidney fibrosis. Kidney International. 2020; 98: 686–698.

[10] Bhattacharya S, Yin J, Huo W, Chaum E. Loss of Prom1 impairs autophagy and promotes epithelial-mesenchymal transition in mouse retinal pigment epithelial cells. Journal of Cellular Physiology. 2023; 238: 2373–2389.

[11] Jiang L, Xu L, Mao J, Li J, Fang L, Zhou Y, *et al*. Rheb/mTORC1 signaling promotes kidney fibroblast activation and fibrosis. Journal of the American Society of Nephrology: JASN. 2013; 24: 1114–1126.

[12] Wang Y, Tang S, Wu Y, Wan X, Zhou M, Li H, *et al*. Upregulation of 6-phosphofructo-2-kinase (PFKFB3) by hyperactivated mammalian target of rapamycin complex 1 is critical for tumor growth in tuberous sclerosis complex. IUBMB Life. 2020; 72: 965–977.

[13] Zhou Z, Plug LG, Patente TA, de Jonge-Muller ESM, Elmagd AA, van der Meulen-de Jong AE, *et al*. Increased stromal PFKFB3-mediated glycolysis in inflammatory bowel disease contributes to intestinal inflammation. Frontiers in Immunology. 2022; 13: 966067.

[14] Song C, Wang S, Fu Z, Chi K, Geng X, Liu C, *et al*. IGFBP5 promotes diabetic kidney disease progression by enhancing PFKFB3-mediated endothelial glycolysis. Cell Death & Disease. 2022; 13: 340.

[15] Yang Q, Huo E, Cai Y, Zhang Z, Dong C, Asara JM, *et al*. PFKFB3-Mediated Glycolysis Boosts Fibroblast Activation and Subsequent Kidney Fibrosis. Cells. 2023; 12: 2081.

[16] Li R, Guo Y, Zhang Y, Zhang X, Zhu L, Yan T. Salidroside Ameliorates Renal Interstitial Fibrosis by Inhibiting the TLR4/NF-κB and MAPK Signaling Pathways. International Journal of Molecular Sciences. 2019; 20: 1103.

[17] Livak KJ, Schmittgen TD. Analysis of relative gene expression data using real-time quantitative PCR and the 2(-Delta Delta

C(T)) Method. Methods (San Diego, Calif.). 2001; 25: 402–408.
[18] Liu L, Wang Y, Yan R, Liang L, Zhou X, Liu H, *et al*. BMP-7 inhibits renal fibrosis in diabetic nephropathy via miR-21 down-regulation. Life Sciences. 2019; 238: 116957.
[19] Pan Z, Yang K, Wang H, Xiao Y, Zhang M, Yu X, *et al*. MFAP4 deficiency alleviates renal fibrosis through inhibition of NF-κB and TGF-β/Smad signaling pathways. FASEB Journal: Official Publication of the Federation of American Societies for Experimental Biology. 2020; 34: 14250–14263.
[20] Chen H, Qi Q, Wu N, Wang Y, Feng Q, Jin R, *et al*. Aspirin promotes RSL3-induced ferroptosis by suppressing mTOR/SREBP-1/SCD1-mediated lipogenesis in PIK3CA-mutant colorectal cancer. Redox Biology. 2022; 55: 102426.
[21] Chen W, Zhang J, Zhong W, Liu Y, Lu Y, Zeng Z, *et al*. Anlotinib Inhibits PFKFB3-Driven Glycolysis in Myofibroblasts to Reverse Pulmonary Fibrosis. Frontiers in Pharmacology. 2021; 12: 744826.
[22] Zhu XJ, Gong Z, Li SJ, Jia HP, Li DL. Long non-coding RNA Hottip modulates high-glucose-induced inflammation and ECM accumulation through miR-455-3p/WNT2B in mouse mesangial cells. International Journal of Clinical and Experimental Pathology. 2019; 12: 2435–2445.
[23] Szwed A, Kim E, Jacinto E. Regulation and metabolic functions of mTORC1 and mTORC2. Physiological Reviews. 2021; 101: 1371–1426.
[24] Wang W, Zhang Y, Huang W, Yuan Y, Hong Q, Xie Z, *et al*. Alamandine/MrgD axis prevents TGF-β1-mediated fibroblast activation via regulation of aerobic glycolysis and mitophagy. Journal of Translational Medicine. 2023; 21: 24.
[25] Chen C, Zhang X. Glycolysis regulator PFKP induces human melanoma cell proliferation and tumor growth. Clinical & Translational Oncology: Official Publication of the Federation of Spanish Oncology Societies and of the National Cancer Institute of Mexico. 2023; 25: 2183–2191.
[26] Humphreys BD. Mechanisms of Renal Fibrosis. Annual Review of Physiology. 2018; 80: 309–326.
[27] Zagory JA, Fenlon M, Dietz W, Zhao M, Nguyen MV, Trinh P, *et al*. Prominin-1 Promotes Biliary Fibrosis Associated With Biliary Atresia. Hepatology (Baltimore, Md.). 2019; 69: 2586–2597.
[28] Short C, Zhong A, Xu J, Mahdi E, Glazier A, Malkoff N, *et al*. TWEAK/FN14 promotes profibrogenic pathway activation in Prominin-1-expressing hepatic progenitor cells in biliary atresia. Hepatology (Baltimore, Md.). 2023; 77: 1639–1653.
[29] Sun Y, Cai H, Ge J, Shao F, Huang Z, Ding Z, *et al*. Tubule-derived INHBB promotes interstitial fibroblast activation and renal fibrosis. The Journal of Pathology. 2022; 256: 25–37.
[30] Kuma A, Tamura M, Otsuji Y. Mechanism of and Therapy for Kidney Fibrosis. Journal of UOEH. 2016; 38: 25–34.
[31] Zhou S, Yin X, Mayr M, Noor M, Hylands PJ, Xu Q. Proteomic landscape of TGF-β1-induced fibrogenesis in renal fibroblasts. Scientific Reports. 2020; 10: 19054.
[32] Yu H, Zhu J, Chang L, Liang C, Li X, Wang W. 3-Bromopyruvate decreased kidney fibrosis and fibroblast activation by suppressing aerobic glycolysis in unilateral ureteral obstruction mice model. Life Sciences. 2021; 272: 119206.
[33] Wei Q, Su J, Dong G, Zhang M, Huo Y, Dong Z. Glycolysis inhibitors suppress renal interstitial fibrosis via divergent effects on fibroblasts and tubular cells. American Journal of Physiology. Renal Physiology. 2019; 316: F1162–F1172.
[34] Li L, Galichon P, Xiao X, Figueroa-Ramirez AC, Tamayo D, Lee JJK, *et al*. Orphan nuclear receptor COUP-TFII enhances myofibroblast glycolysis leading to kidney fibrosis. EMBO Reports. 2021; 22: e51169.
[35] He X, Cantrell AC, Williams QA, Chen JX, Zeng H. TIGAR deficiency sensitizes angiotensin-II-induced renal fibrosis and glomerular injury. Physiological Reports. 2022; 10: e15234.
[36] Yang Q, Huo E, Cai Y, Zhang Z, Dong C, Asara JM, *et al*. Myeloid PFKFB3-mediated glycolysis promotes kidney fibrosis. Frontiers in Immunology. 2023; 14: 1259434.
[37] VanHook AM. Metabolic dysregulation into fibrosis. Science. 2019; 366: 1467–1469.
[38] Nakano T, Watanabe H, Imafuku T, Tokumaru K, Fujita I, Arimura N, *et al*. Indoxyl Sulfate Contributes to mTORC1-Induced Renal Fibrosis via The OAT/NADPH Oxidase/ROS Pathway. Toxins. 2021; 13: 909.